A Cross-Layer Solution for Ultrawideband Based Wireless Video Sensor Networks

L. Campelli
CEFRIEL
Politecnico di Milano
Milan 20133, Italy
Email: Luca.Campelli@cefriel.it

I. F. Akyildiz
Broadband Wireless Networking Laboratory
Georgia Institute of Technology
Atlanta, GA 30332, USA
Email: ian@ece.gatech.edu

L. Fratta, M. Cesana
Dipartimento di Elettronica e Informazione
Politecnico di Milano
Milan 20133, Italy
Email: {fratta, cesana}@elet.polimi.it

***Abstract*—A cross-layer communication protocol called VSN-Module is introduced for Wireless Video Sensor Networks based on UltraWideBand (UWB) radio technology at the physical layer. The core of our solution is a distributed path reservation scheme which routes video traffic from sources (sensors) to a sink. The path establishment takes into account the specific requirements of video flows such as bandwidth, end-to-end delay and jitter, as well as the current status of the traversed devices such as the available bandwidth, the energy consumption, and the quality of the wireless channels. Simulation experiments are carried out and the performance of the VSN-Module is evaluated in terms of maximum end-to-end delivery delay, maximum delay jitter, and power consumption, under different video flow requirements.**

I. Introduction

Wireless Video Sensor Networks (WVSNs) are composed of interconnected, battery-powered miniature video cameras, each packed with a low-power wireless transceiver that is capable of processing, sending, and receiving data. Video sensors will be used to enhance and complement existing surveillance systems against crime and terrorist attacks. Large scale networks of video sensors can extend the ability of law enforcement agencies to monitor areas, public events, private properties and borders. There exist several other applications of WVSNs [1].

Several of these applications require the sensor network paradigm to be re-thought in view of the need for mechanisms to deliver video content with a certain level of Quality of Service (QoS). Since the need to minimize the energy consumption has driven most of the research in sensor networks so far, mechanisms to efficiently deliver application-level QoS, and to map these requirements to network-layer metrics such as latency and jitter, have not been primary concerns in mainstream research on classical sensor networks. Moreover, the challenging goal of delivering video over resource-limited infrastructure requires a wise optimization of all the communication protocols involved in the process. To this end, a cross-layer approach is highly favorable.

Cross-layering in WSNs has been recently becoming an effective alternative solution to traditional layered protocol architectures. Cross-layering stands for joint design of network protocols, with the clear advantages over layered protocol design in terms of limited overhead and possibility to optimize jointly different protocol functionalities. Although several papers are focused on cross-layer design [2], a systematic methodology to accurately model and leverage cross-layer interactions is still missing. Most of the existing studies [3][4] decompose the resource allocation problem at different layers, and consider allocation of the resources at each layer separately. In many other cases [5][6][7], resource allocation problems are treated either heuristically, or without considering cross-layer interdependencies, or by considering pairwise interactions between isolated pairs of layers.

In this paper we introduce the Video Sensor Networks Module *VSN-Module*, a cross-layer communication protocol which provides QoS support. The *VSN-Module* is based on a distributed path reservation scheme, which is able to set up multi-hop routes from the video traffic source to the traffic sink, while satisfying the flow requirements (bandwidth, end-to-end delay, delay jitter). *VSN-Module* is designed according to a cross-layer solution of different protocol functionalities in different layers.

Due to the high bandwidth requirements of video applications, we argue that the physical layer must be integrated into (and exploited by) the upper layer functionalities of medium access, routing and transport layer. Thus, the *VSN-Module* adopts the Ultrawideband (UWB) technology at the physical layer, and couples the channel access with the physical transmission parameters.

The main contribution of our work is the development of a cross layer communication protocol module to support video flows in energy and resource constrained video sensor networks. In particular, we propose:

- a cross-layer approach capturing the interdependencies and functionalities of medium access control, routing, congestion control and UWB radio transceivers.
- a distributed path reservation scheme for video flows.

The remainder of the paper is organized as follows. In Section II, we present the network architecture and the feature of the video applications. In Section III we explain the functionalities of the *VSN-Module*, whose performance is evaluated in Section IV. Our concluding remarks are given in Section V.

II. Network Architecture

We refer to heterogeneous and hierarchical network scenarios where sensor nodes are distinguished for the type of

978-1-4244-2324-8/08/$25.00 © 2008 IEEE.

This full text paper was peer reviewed at the direction of IEEE Communications Society subject matter experts for publication in the IEEE "GLOBECOM" 2008 proceedings.

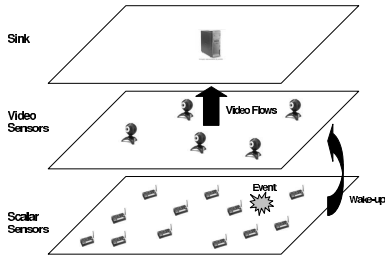

Fig. 1. *Three-Tier Architecture used in VSN-Module.*

hardware and for the specific networking capabilities. Namely, we consider the multi-tier architecture shown in Figure 1, where resource-constrained, low-power elements are in charge of performing simple tasks, such as detecting scalar physical measurements, while more powerful devices (e.g., geared with cameras) can take on more complex tasks [8].

In this paper, we focus on video streaming applications with stringent delay requirements leveraging the traffic classification provided in [1]. Quantitatively, we assume the maximum end-to-end delay allowed for video packets to be 200ms [9]. Such delay bound includes both the delivery and the playback delays at the destination. We note that the playback delay needs to be dimensioned on the maximum delay jitter J^{max}.

Besides the sensing capabilities (either scalar sensing, or video cameras), the quality of the video streaming application depends on the specific wireless technology to set up the communications among sensors. Among the potential alternative technologies, we focus on UWB, which enables high data rates, low power consumption and low-cost hardware [10].

We assume that all devices in Figure 1 are equipped with UWB radio technology, and run the *VSN-Module*. In particular, we consider the Time-Hopping Impulse Radio UWB (TH-IR-UWB) [10]. The time is slotted in chips of duration T_c, which are organized in frames of the length $T_f = N_h T_c$ chips, where N_h is the number of chips per frame. A sensor transmits one pulse in one chip per frame. Binary Pulse Position Modulation (2-PPM) is used within the chips. Multiuser access is provided by pseudo-random Time Hopping Sequence (THS) that determines in which chip each user should transmit reducing the interference due to concurrent transmissions. Furthermore, a repetition code N_s is introduced. It represents the number of pulses used for the transmission of the same information bit. The resulting channel bit rate is thus $R_b = \frac{1}{N_s N_h T_c} \quad [bps]$.

III. VSN-Module Description

The *VSN-Module* defines a distributed technique for the reservation of paths for video traffic, incorporating access, routing, and congestion control functionalities. Path reservation is done on a hop-by-hop fashion through a distributed negotiation procedure between traffic source/relayer and the next-hop candidates. The outcome of this negotiation is the choice of the "best" next-hop for the given flow depending on traffic characteristics and quality of service requirements, energy level of the potential relaying sensor, and the quality of the wireless link. The cross-layer negotiation exploits UWB error protection (N_s) in order to perform error control functionalities.

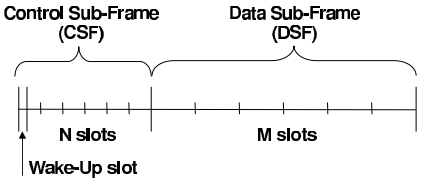

Fig. 2. *The VSN-Module's logical frame structure.*

To ease up the comprehension of the protocol, we split its description into different components.

A. VSN-Module Framing

VSN-Module uses a dynamic Time Division Multiple Access (TDMA) scheme, where each frame is divided into two sub-frames: a *Control Sub-Frame* (CSF) and a *Data Sub-Frame* (DSF). Figure 2 shows the logical frame structure. We assume that the frame and slot synchronization is realized using solutions like those proposed in [11][12]. The CSF is organized in N slots plus a wake-up slot during which all sensors are forced to stay active. Sensors willing to trigger signaling procedures send out a tone in the wake-up slot.

In CSF, sensors accomplish several operations including: spreading of information on the network topology and the current resource assignment to neighboring nodes, exchanging of signalling information to reserve multi-hop routes for real-time video traffic, acknowledging video transmissions.

To this end, each sensor has to acquire a resource (i.e., a slot) in the CSF, which can be used to spread all the wanted signalling information. The acquisition procedure is based on the RR-ALOHA protocol [13]. In detail, when a new sensor enters the network, it sends a tone in the wake-up slot which is received by its neighboring nodes. Sensors receiving such tone activate and send out a *Spread Neighbor Packet* (SNP) in their own CSF slot. Each SNP contains channel status information as perceived by the sender. The accessing sensor can then obtain the current channel status (occupied/unoccupied slots in the CSF) by merging all the received SNPs. Those slots which are not occupied by one-hop and two-hop neighbors can be used by the accessing sensor. The accessing sensor has to wait for an acknowledgment from all of its neighbors, which will eventually come in the following CSF. If the access has been successful, the new sensor stops sending tones in the wake-up slot and moves to the sleep state. The procedure described so far is effective in establishing reliable one-hop broadcast channels which can be used to implement the signalling procedures for reserving resources in the DSF for the video transmissions.

The DSF has M slots and is used to carry video traffic. Each sensor is assigned a portion of bandwidth composed of a set of time slots to receive data. We call this a Reception Schedule (RS). Each sensor periodically wakes up during its reception schedule to check for any data transmission. RS assignment is realized through the reliable broadcast channels provided within the CSF. Indeed, the SNP messages also contain information on the current RS, i.e., indicating the slots selected for reception by the SNP transmitter. Consequently, each sensor receiving SNPs from its neighbors can obtain

This full text paper was peer reviewed at the direction of IEEE Communications Society subject matter experts for publication in the IEEE "GLOBECOM" 2008 proceedings.

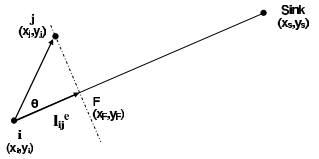

Fig. 3. *The effective length of forwarding between i and j.*

information on the occupation of the DSF also, consequently being able of choosing available RSs for itself, i.e., RSs which do not overlap with those of the one-hop neighbors.

If the raw data rate of time slot k in the RS is R_k, we have:

$$R_k = \frac{L_D}{NL_C + ML_D + L_W} R_b, \tag{1}$$

where L_D is the data slot dimension (in bits) while L_C, and L_W are the control and wake up slot dimensions. As a consequence, the total available bandwidth in reception assigned to a single sensor is:

$$B_{RS} = \sum_{k=1}^{K} R_k, \tag{2}$$

where K is the number of time slots in the RS.

B. Source and Relay Node Operations

We call i the source or relay sensor node which handles the video flow m. Each sensor i knows the destination and its position, and further retrieves the following information for each of its neighbors: the ID, j, and the geographical position, (x_j,y_j). We call C_i the set of i's neighbors ($j \in C_i$). Each sensor is able to classify each packet belonging to video flow m according to the following parameters:the priority level, p_m, to distinguish among different video flows, the flow rate, f_m in *bps*, the time of connection, T_m^{max} in s, and the delivery delay budget left, D_m^{max} in s.

From the set C_i, sensor i orders a list of *Feasible Next Hops* (FNHs) for video flow m packets according to the *effective length metric* [5], which represents the advancement of information in a single-hop towards the destination. Figure 3 shows the effective length for the transmission from i to j, l_{ij}^e, which is: $l_{ij}^e = \cos\theta \; |\overrightarrow{ij}|$. If l_{ij}^e is negative, the neighbor j is dropped from FNHs list.

The source or relay sensor node starts the negotiation phase by sending on the broadcast channel of the CSF a *Request To Forward* (RTF) packet containing: the ordered FNHs list and the quality of service parameters of the flow and setting a Time Out interval equal to the frame size. When the Time Out expires, node i selects the best next-hop among the subset of neighbors belonging to FHN which are able to support the video flow.

If no sensor replies to the RTF packet, the relay sensor immediately retransmits an RTF packet including also neighbors with negative effective length to increase the probability of finding alternative paths to the sink.

C. Next-Hop Candidate Operations

Upon reception of an RTF, each sensor whose identifier is stored in the RTF itself, decides whether to answer to the RTF or not. Such a decision is based on cross-layer parameters, and can be summarized in the following binary function which returns the *Cross Layer Availability*, $\mathcal{A}$, of the specific sensor.

The $\mathcal{A}$ function is defined as:

$$\mathcal{A} = \begin{cases} 1, & \text{if } \begin{cases} E_j^{tot} \geq \gamma(f_m T_m^{max}(e^{tx} + e^{rx})) + 2E^{neg} \\ \exists\, S \subseteq RS_j \mid \sum_{k \in S} R_k^{eff}(i,j) \geq \frac{f_m}{\rho} \\ G_j \geq G_{min} \\ PQ_{th} \geq PQ_j \end{cases} \\ 0, & \text{otherwise} \end{cases} \tag{3}$$

If $\mathcal{A}$ returns 1, all the conditions to become a relay node for packets belonging to flow m are satisfied. In this case, the neighbor j will send back an *Available To Forward* (ATF) packet. The meaning of each condition is explained in the next subsections from III-C.1 to III-C.3.

C.1) Energy Constraint

The first condition in Equation (3) estimates the energy consumed to handle the incoming flow m. If the remaining energy of the sensor E_j^{tot} is greater than the energy needed to handle the flow, the first condition is satisfied.

$f_m T_m^{max}(e^{tx} + e^{rx})$ represents the amount of energy in order to receive and relay packets of a given flow. γ is the *retransmission factor* and represents the average number of transmissions needed to deliver the video flow packets, while e^{tx} and e^{rx} are the energy per bit consumed during the transmission and reception of a single video flow packet. γ obviously depends on several factors including network topology, traffic rates and interference, thus it must be dynamically set according to the current network conditions. Finally, E^{neg} is the energy spent during the negotiation phase.

C.2) UWB Error Control and Resource Allocation

The purpose of the UWB error control and reservation functionality is twofold:

- it introduces an error control mechanism to protect video packets transmission from bad channel conditions.
- it actually reserves the required bandwidth, i.e., it selects those time slots in the RS which are reserved to receive the incoming video flow.

Due to wireless channel impairments such as fast fading, slow shadowing and interference, the actual data rate associated with the single slot in the RS may be lower than the nominal one. Furthermore, depending on the current propagation condition, the number of corrupted bits in each time slot can become unacceptable. Thus, we believe that the bandwidth reservation mechanism must be able to account for the current wireless channel conditions, when reserving bandwidth.

VSN-Module performs channel estimation for each time slot in the RS and introduces the required redundancy in the time slot in order to keep the BER below a given threshold (BER_{th}).

If we consider the bandwidth negotiation between sensor i and j, the channel estimation runs as follows: in the RTF packet the sensor i reports the power level used during the RTF transmission, $P_{tx}^{CSF}(i)$. When sensor j decodes the RTF

packet, it estimates the Signal To Noise Ratio $\widehat{SNR^{CSF}}(i,j)$ and the total power detected, $\widehat{P_{tot}^{CSF}}(i,j)$. We link such parameters to the thermal noise σ_n^2, the interfering power $P_I^{CSF}(i,j)$ and the power received by j P_{rx}(i,j) as follows:

$$\widehat{SNR^{CSF}}(i,j) \cong \frac{P_{rx}^{CSF}(i,j)}{\sigma_n^2 + P_I^{CSF}(i,j)} \quad (4)$$

$$\widehat{P_{tot}^{CSF}}(i,j) \cong P_{rx}^{CSF}(i,j) + P_I^{CSF}(i,j) + \sigma_n^2 \quad (5)$$

From equations (4) and (5), we have:

$$\widehat{P_{rx}^{CSF}}(i,j) = \frac{\widehat{SNR^{CSF}}(i,j)}{\widehat{SNR^{CSF}}(i,j)+1} \widehat{P_{tot}^{CSF}}(i,j), \quad (6)$$

consequently, the attenuation gain $\widehat{\beta^{CSF}}(i,j)$ can be estimated as:

$$\widehat{\beta^{CSF}}(i,j) = \frac{\widehat{P_{rx}^{CSF}}(i,j)}{P_{tx}^{CSF}(i)} \quad (7)$$

Sensor j also measures the amount of background interference in each available RS$_j$ slot as: $\widehat{P_I^{DSF(k)}}(.,j)$ with $k \in RS_j$. If we assume channel conditions vary slowly, then the changes inside a logical frame are negligible and therefore $\widehat{\beta^{DSF}}(i,j) \cong \widehat{\beta^{CSF}}(i,j)$.

The estimation of all previous parameters allows to decide the redundancy factor N_s^k(i,j) for each available slot of RS$_j$ over the link (i,j). Indeed, sensor j is able to predict the SNR obtainable if sensor i transmits over the available slot k:

$$\widehat{SNR^{DSF(k)}}(i,j) = \frac{\widehat{\beta^{DSF}}(i,j) P_{tx}^{CSF}(i)}{\widehat{P_I^{DSF(k)}}(.,j)} \quad (8)$$

In (8) we consider $P_{tx}^{DSF}(i) \cong P_{tx}^{CSF}(i)$. Given the SNR estimated, assuming Gaussian Approximation [14] and a 2-PPM modulation, we may estimate the (BER) as a function of the redundancy factor N_s^k(i,j) as follows:

$$BER^{DSF(k)}(i,j) = \frac{1}{2} erfc\left(N_s^k(i,j) \sqrt{\widehat{SNR^{DSF(k)}}(i,j)} \right) \quad (9)$$

Equation (9) allows to determine N_s^k(i,j) to meet the constraint $BER^{DSF(k)}(i,j) \leq BER_{th}$. If the required $N_s^k(i,j)$ is above a given threshold, N_s^{th}, sensor j decides not to use k for the bandwidth allocation of i.

The actual bandwidth associated with the time slot k in the RS$_j$ is consequently calculated as: $R_k^{eff}(i,j) = R_k / N_s^k(i,j)$. A video flow can be supported by the current FNH if there exists at least a subset S$_j$ of time slots in the RS$_j$, i.e., a schedule, such that:

$$\sum_{k \in S} R_k^{eff}(i,j) \geq \frac{f_m}{\rho}, \quad (10)$$

where the parameter ρ defines a margin in the assigned bandwidth.

If the FNH (*Feasible Next Hop*) receives multiple RTFs carrying requests for multiple video flows, the higher priority flows are assigned the bandwidth first, and, in case of equal priority flows, the priority is given to flows with lower delivery delay budgets left D_m^{max}.

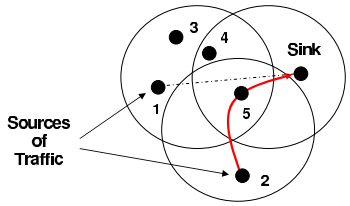

Fig. 4. *Example of RTF/ATF Negotiation in VSN-Module.*

C.3) Connectivity Constraint and Local Congestion Control

The third condition in Equation (3) is meant for favoring those FNHs which have a larger number of neighbors. The intuition is that for lesser neighbors the smaller is the probability of finding good routes to the sink. G_j is the current number of neighbors of FNH j and G_{min} is the threshold.

The condition $PQ_{th} \geq PQ_j$ performs a local congestion control. Since a sensor receives video flows only if it indicates to be a possible candidate as the next-hop, the congestion constraint checks if the number of all data packets in sensor j, PQ_j, is below the Packet Queueing threshold, PQ_{th}. Otherwise, the sensor j will not send any ATF (*Available to Forward*) packet.

D. Path Reservation Example

In Figure 4, we give an example of *VSN-Module* operation mode. For the sake of simplicity, we assume that sensors have no constraints on energy, buffering capabilities i.e., $PQ_{th} \rightarrow \infty$ in Eq. (3) and the available connectivity $G_{min} = 1$ in Eq. (3). Moreover, we assume that a video flow originates at sensor 2 (m=2), traverses sensor 5 and reaches the sink.

The RS of sensor 5 is fully assigned to the flow, i.e., 5 does not have any available resources for new incoming flows.

Let us assume that Sensor 1 wants to set up a video flow to the sink. It broadcasts an RTF packet carrying the flow requirements which has to be delivered (say flow m=1), and the list of potential FNHs in descending order from the closest to the sink, according to the effective transmission length defined in Eq. (3). In this case the ordered list is {5, 4, 3}.

As soon as sensors 3, 4, and 5 receive sensor 1's RTF, they check the FNH list, and run the $\mathcal{A}$ control (Eq. (3)). Neighbors 3 and 4 will obtain $\mathcal{A}$=1, since they actually have enough bandwidth to allocate to the incoming flow according to Eq. (10). They will consequently reply with ATF packets. On the other hand, sensor 5 does not have enough bandwidth to reserve for the incoming flow, thus it will not send any ATF because the condition in Eq. (10) is not satisfied.

Upon reception of the ATFs, sensor 1 will choose sensor 4 as the next hop, and it will soon start transmitting video contents to 4 according to the schedule specified by 4 in its own ATF. In turn, sensor 4 will perform the very same procedure to relay the video traffic to the sink.

IV. Performance Evaluation

Having in mind the assumptions taken in Sections II on *network topology*, *traffic sources* and *traffic priorities*, we have tested the performance of *VSN-Module* through detailed simulations in ns2 [15]. We have implemented the *VSN-Module* and UWB physical layer, and added them to the basic

This full text paper was peer reviewed at the direction of IEEE Communications Society subject matter experts for publication in the IEEE "GLOBECOM" 2008 proceedings.

TABLE I
Video flows generated by video sensors in the VSN-Module scenario.

Name	Frame Rate [frames/s]	Resolution [pixels^2]	Color Depth [bits/pixels]	Flow [kbps]
RGB-32	15	32x32	16 (RGB)	245.76
Mono-64	15	64x64	8 (Monochrome)	491.52
RGB-64	10	64x64	16 (RGB)	655.36

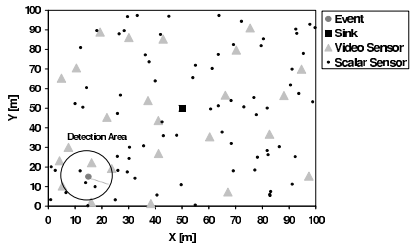

Fig. 5. *Network topology used in the simulations. Squares represent the sink of video flows, triangles are video sensors, and dots are scalar sensors.*

functionalities of the network simulator. We assume that video sensors are equipped with CMOS camera ADCM-1700 and Cyclops processor [16], which is able to adapt the raw video information generated by the CMOS camera by generating different quality video streams, depending on the resolution, the frame rate and color depth. Table I presents the features of video flows used in our simulations, whereas Figure 5 shows the reference network topology featuring 100 sensors of different type (as reported in the figure). Here, an event activates scalar sensors within a detection circular range at the bottom left corner of the figure and they trigger video sensors in the neighborhood. Upon activation, video sensors start to generate video flows directed to the sink in the middle. Table II reports the standard configuration of the UWB/TDMA physical layer.

All the results presented in this section have been obtained averaging over 50 simulations for each realization of the network instance, unless differently specified. The measured confidence intervals for all collected statistics are below 5% in 98% of all cases.

VSN-Module has several input parameters which influence its performance. The purpose of this section is to analyze the impact of these parameters on the performance of video applications, thus providing qualitative guidelines for the dimensioning of the VSN-Module. We evaluate the quality of real-time video flows using the delivery probability, the maximum end-to-end delivery delay, the maximum jitter delay and the consumed power. In Table III we show the set of parameters and the values used in the simulations.

As pointed out in Section II, a reasonable requirement for real-time video traffic in terms of maximum end-to-end delay E^{max} is: $E^{max} = D^{max} + J^{max} \leq 200ms$, where D^{max} and J^{max} are the maximum delivery delay and the maximum jitter delay, respectively.

TABLE II
Standard Setting of the simulation parameters related to the UWB radio interface and the TDMA structure.

Parameter	Value	Parameter	Value
R_b	37.70 Mbps	P_{sl}	33.33 nW
Radio Range	20 m	N	40
Sense Range	20 m	M	40,50,...,100
Con. Pow. P_{tx}	165 μW	Data Slot (L_D)	1000 bytes
Cons. Pow. P_{rx}	90 μW	Control Slot (L_C)	600 bytes
Cons. Pow. P_{id}	90 μW	Wake-Up Slot (L_W)	30 bytes

TABLE III
VSN-Module Parameters

Parameter	Value	Parameter	Value
N_s^{th}	3	K^{Sink}	12,13,...,20
γ	2	ρ	0.3,0.4,...,1
BER_{th}	10^{-2}	G_{min}	1
K	6		

The first parameter we want to dimension is the frame length as shown in Figure 2. The value N, the number of slots in the signalling subframe, is strictly bounded by the number of all sensors in two-hop clusters since each of them needs a unique signalling slot. Hence, N mainly depends on the topology of the specific WVSNs. The value M, the number of slots in data subframe, is strictly related to the type of application traffic to be delivered and must account for the tradeoff between capacity, energy consumption, and delivery delay. Roughly speaking, setting high values of M decreases the actual data rate offered at reception and increases the average delivery delay, but, on the other hand, it reduces power consumption.

Figures 6 and 7 show the maximum end-to-end delay and the power consumed versus M for different classes of multimedia traffic, respectively. All configurations provide 100% delivery probability except for RGB-64 when M=40. The results confirm that when M increases, the power consumption reduces (Figure 7) and the maximum end-to-end delay increases (Figure 6). The curves in Figure 6 can be used to dimension the parameter M for each type of video flows by choosing the maximum values with E^{max} below the required threshold (200ms in the figure).

Upon choosing the frame length, the performance of the *VSN-Module* is affected by the actual bandwidth available for traffic reception at each sensor (see Eq. 2). In particular, since the video traffic sink represents a potential bandwidth bottleneck, it is worth dimensioning the bandwidth allocated at the sink itself. Figure 8 shows for $M = 50$ the delivery probability versus K^{Sink}, the sink's bandwidth (the number of reserved slots for reception).

The delivery probability increases with K^{Sink} up to a maximum value obtained for K^{Sink}=16 in Figure 8. Increasing K^{Sink} beyond this value decreases the delivery probability since too much bandwidth is allocated to the sink and the surrounding sensors start starving. In fact, the slots allocated to the sink cannot be reused by the sensors.

A significant contribution to E^{max} is given by the jitter delay, J^{max}, suffered by the video packets waiting for transmission in the sensor buffers. J^{max} highly depends on the available bandwidth at each *VSN-Module*. For the case M=50 and K^{max}=16, we have measured J^{max} as a function of ρ, resource utilization parameter. We observe, in Figure 9, that for high bandwidth demand flows (Mono-64 and RGB-64) J^{max} decreases with ρ. Unfortunately, low values of ρ require more bandwidth margin, hence, the available bandwidth at each sensor might not be enough (see Figure 10) This effect has an impact on the delivery probability which drastically drops when ρ decreases due to the bandwidth starvation.

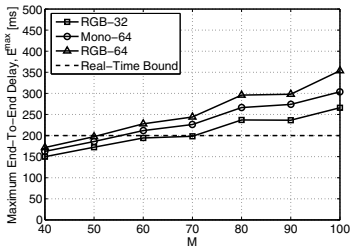

Fig. 6. *Maximum End-To-End Delay versus M for different classes when K=6, K^{Sink}=12 and ρ=0.9.*

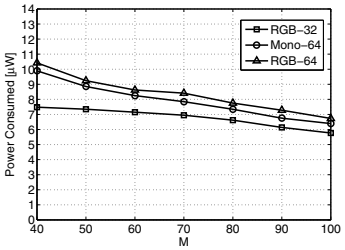

Fig. 7. *Power Consumed versus M for different classes when K=6, K^{Sink}=12 and ρ=0.9.*

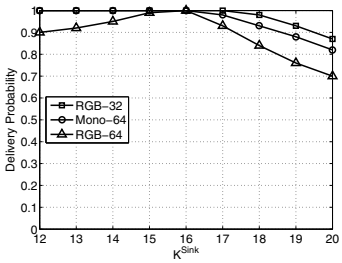

Fig. 8. *Delivery Probability versus K^{Sink} for different classes when K=6, M=50 and ρ=0.9.*

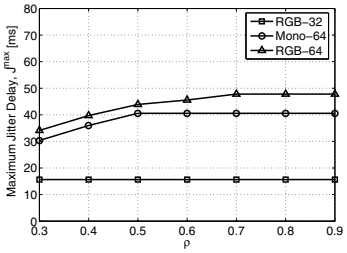

Fig. 9. *Maximum Delay Jitter versus ρ for different classes when M=50, K=6 and K^{Sink}=16.*

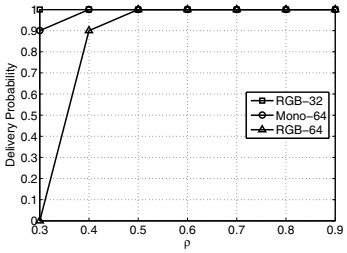

Fig. 10. *Delivery Probability versus ρ for different classes when M=50, K=6 and K^{Sink}=16.*

In this scenario, our investigation shows that a qualitatively good value of ρ is 0.5, provides the lowest jitter delay, while guaranteeing delivery probability equal to 1. For less bandwidth demanding flows (e.g., RGB-32) such effect is not critical (see Figure the 9) since sensors never get congested and the delivery probability remains always high (Figure 10).

V. Conclusion

In this paper, we addressed the problem of delivering real-time video traffic in WSNs. Having in mind a multi-tier architecture composed by scalar, video sensors and a sink as final destination, we proposed the *VSN-Module*, a cross-layer solution based on UltraWideBand radio technology which is able to build up routes to the sink, satisfying video flow constraints. In the *VSN-Module*, UWB enables error control functionalities which protect video packets from wireless channel impairments such as fading holes and cumulative interferences.

We have evaluated through simulation the impact of *VSN-Module* parameters on the perceived quality of real-time video traffic, and we have provided general guidelines to dimension *VSN-Module* parameters to support different types of video streams. The achieved results show that the cross-layering approach adopted by *VSN-Module* is effective in reserving multi-hop paths to remotely deliver video traffic.

References

[1] I. F. Akyildiz, T. Melodia, and K. R. Chowdhury, "A survey on wireless multimedia sensor networks," *Elsevier Computer Networks Journal*, vol. 51, no. 4, pp. 921–960, March 2007.

[2] I. F. Akyildiz, M. C. Vuran, and O. B. Akan, "A cross-layer protocol for wireless sensor networks," in *proceedings of Conference on Information Sciences and Systems (CISS)*, March 2006.

[3] S. Cui, R. Madan, A. Goldsmith, and S. Lall, "Joint routing, mac, and link layer optimization in sensor networks with energy constraints," in *proceedings of IEEE International Conference on Communications (ICC)*, May 2005, pp. 725–729.

[4] R. Madan, S. Cui, S. Lall, and A. Goldsmith, "Cross-layer design for lifetime maximization in interference-limited wireless sensor networks," in *proceedings of IEEE Conference on Computer Communications (INFOCOM)*, March 2005, pp. 1964–1975.

[5] M. Zorzi and R. Rao, "Geographic random forwarding (geraf) for ad hoc and sensor networks: Energy and latency performance," *IEEE Transaction on Mobile Computing*, vol. 2, no. 4, pp. 349–365, October-December 2003.

[6] K. Seada, M. Zuniga, A. Helmy, and B. Krishnamachari, "Energy-efficient forwarding strategies for geographic routing in lossy wireless sensor networks," in *proceedings of ACM Conference on Embedded Networked Sensor Systems (Sensys)*, November 2004, pp. 108–121.

[7] M. C. Vuran, V. B. Gungor, and O. B. Akan, "On the interdependency of congestion and contention in wireless sensor networks," in *proceedings of ICST SemMetrics*, July 2005.

[8] P. Kulkarni, D. Ganesan, and P. Shenoy, "The case for multitier camera sensor network," in *proceedings of ACM Workshop on Network and Operating System Support for Digital Audio and Video (NOSSDAV)*, June 2005, pp. 141–146.

[9] G. Karlsson, "Asynchronous transfer of video," *IEEE Communication Magazine*, vol. 34, no. 8, p. 118126, August 1996.

[10] M. Z. Win and R. A. Scholtz, "Ultra-wide bandwidth time-hopping spread-spectrum impulse radio for wireless multiple-access communications," *IEEE Transaction on Communications*, vol. 48, no. 4, pp. 679–691, April 2000.

[11] Q. Li and D. Rus, "Global clock synchronization in sensor networks," *IEEE Transaction on Computers*, vol. 55, no. 2, pp. 214–226, February 2006.

[12] W. Su and I. F. Akyildiz, "Time-diffusion synchronization protocol for wireless sensor networks," *IEEE/ACM Transaction on Networking*, vol. 13, no. 2, pp. 384–397, April 2005.

[13] F. Borgonovo, A. Capone, M. Cesana, and L. Fratta, "Adhoc mac: New mac architecture for ad hoc networks providing efficient and reliable point-to-point and broadcast services," *ACM Wireless Networks*, vol. 10, no. 4, pp. 359–366, July 2004.

[14] G. Durisi and G. Romano, "On the validity of gaussian approximation to characterize the multiuser capacity of uwb th ppm," in *proceedings of IEEE Conference on Ultra Wideband Systems and Technologies*, May 2002, pp. 151–161.

[15] Http://www.isi.edu/nsnam/ns/.

[16] M. Rahimi, D. Estrin, R. Baer, H. Uyeno, and J. Warrior, "Cyclops, image sensing and interpretation in wireless networks," in *proceedings of ACM Conference on Embedded Networked Sensor Systems (SenSys)*, November 2005, pp. 90–101.